



King's Research Portal

DOI:

[10.1016/j.ijpharm.2021.120442](https://doi.org/10.1016/j.ijpharm.2021.120442)

Document Version

Peer reviewed version

[Link to publication record in King's Research Portal](#)

Citation for published version (APA):

Okwuosa, T. C., Sadia, M., Isreb, A., Habashy, R., Peak, M., & Alhnan, M. A. (2021). Can Filaments be stored as a shelf-item for on-demand manufacturing of oral 3D printed tablets? An initial stability assessment. *INTERNATIONAL JOURNAL OF PHARMACEUTICS*, 600, 120442. [120442].
<https://doi.org/10.1016/j.ijpharm.2021.120442>

Citing this paper

Please note that where the full-text provided on King's Research Portal is the Author Accepted Manuscript or Post-Print version this may differ from the final Published version. If citing, it is advised that you check and use the publisher's definitive version for pagination, volume/issue, and date of publication details. And where the final published version is provided on the Research Portal, if citing you are again advised to check the publisher's website for any subsequent corrections.

General rights

Copyright and moral rights for the publications made accessible in the Research Portal are retained by the authors and/or other copyright owners and it is a condition of accessing publications that users recognize and abide by the legal requirements associated with these rights.

- Users may download and print one copy of any publication from the Research Portal for the purpose of private study or research.
- You may not further distribute the material or use it for any profit-making activity or commercial gain
- You may freely distribute the URL identifying the publication in the Research Portal

Take down policy

If you believe that this document breaches copyright please contact librarypure@kcl.ac.uk providing details, and we will remove access to the work immediately and investigate your claim.

1 Research paper

2

3 **Can Filaments be stored as a shelf-item for on-demand**
4 **manufacturing of oral 3D printed tablets? An initial stability**
5 **assessment**

6

7

8

9 Tochukwu C Okwuosa^{1,2}, Muzna Sadia¹, Abdullah Isreb¹, Rober Habashy¹,
10 Matthew Peak³ Mohamed A Alhnan⁴

11

12

13 ¹*School of Pharmacy and Biomedical Sciences, University of Central Lancashire, Preston PR1 2HE, United Kingdom.*

14 ²*School of Life and Medical Sciences, University of Hertfordshire, AL10 9AB Hatfield, United Kingdom.*

15 ³*Paediatric Medicines Research Unit, Alder Hey Children's NHS Foundation Trust, Liverpool, UK*

16 ⁴*Institute of Pharmaceutical Science, King's College London, London, United Kingdom.*

17

18

19

20 *Corresponding author at:
21 Institute of Pharmaceutical Sciences
22 King's College London
23 150 Stamford Street
24 London SE1 9NH. Tel.: +44 (0)20 7848 7265
25 Email: Alhnan@kcl.ac.uk

26

27 **Abstract**

28 3D printing of oral solid dosage forms is a recently introduced approach for dose personalisation. Fused
29 deposition modelling (FDM) is one of the promising and heavily researched 3D printing techniques in
30 the pharmaceutical field. However, the successful application of this technique relies greatly on the
31 mass manufacturing of physically and chemically stable filaments, that can be readily available as a
32 shelf item to be 3D printed on-demand. In this work, the stability of methacrylate polymers (Eudragit
33 EPO, RL, L100-55 and S100), hydroxypropyl cellulose (HPC SSL) and polyvinyl pyrrolidone (PVP)-
34 based filaments over 6 months were investigated. Filaments manufactured by hot melt extrusion (HME)
35 were stored at either 5 °C or 30 °C + 65 %RH with/without vacuuming. The effects of storage on their
36 dimensions, visual appearance, thermal properties, and ‘printability’ were analysed. Theophylline
37 content, as well as *in vitro* release from the 3D printed tablets were also investigated. The filaments
38 were analysed before storage, then after 1, 3 and 6 months from the manufacturing date.

39 Storing filaments at these conditions had a significant effect on their physical properties such as shape,
40 dimensions, flexibility and hence compatibility with FDM 3D printing. In general, the methacrylate-
41 based filaments were more physically stable and compatible with FDM 3D printing following storage.
42 Owing to their hygroscopic nature, cellulose- and PVP-based filaments demonstrated a reduction in
43 their glass transition temperature upon storage, leading to increased flexibility and incompatibility with
44 FDM 3D printer. Theophylline contents was not significantly changed during the storage.

45 This work provides preliminary data for the impact of polymer species on the long-term stability of the
46 filaments. In general, storage and packaging conditions have major impact on the potential of on-
47 demand manufacturing of 3D printed tablets using hot melt extruded filaments.

48

49 **1. Introduction**

50 For many years, drug dosing for adults were based on the age and weight of the patient, with the
51 dose for children extrapolated linearly from the former. The downside of such approach is the lack of
52 consideration of demographic, genetic, clinical and environmental factors, which proved to contribute
53 to population variabilities (Cella et al. 2010). Hence, varied responses to therapy and susceptibility to
54 adverse drug reactions have always been predominant issues (Al-Metwali and Mulla 2017; Nyboe
55 Andersen et al. 2017). Dose personalisation, therefore, offers the advantage of tailoring doses to the
56 patients' needs when required. With advancements in pharmacogenomics and wearable technologies,
57 there is a rising interest in dose personalisation, in response to tested biomarkers, to achieve target
58 pharmacodynamics and pharmacokinetics profiles.

59 A readily available dosing system will ensure efficient and safe dosing with minimal adverse effects
60 when administered to patients. However, such an approach is mostly applicable currently for
61 injectables, which allows easy dose adjustments (Patel et al. 2014). For this approach to be widely
62 applied, a digital personalisation solution for commonly used dosage forms e.g. tablets should be
63 developed. For tablets, dose adjustments are frequently achieved through the practice of splitting. This
64 approach is reported to introduce dosing inaccuracies (Habib et al. 2014), which could lead to
65 underdosing, overdosing and severe toxicities with certain active pharmaceutical ingredients (APIs).

66 Different approaches are currently being investigated to personalise oral dosage forms, with 3D
67 printing demonstrating significant potential (Isreb et al. 2019; Pereira et al. 2019; Tagami et al. 2019;
68 Sen et al. 2020; Martinez et al. 2018). FDM has been heavily researched as an effective and accessible
69 3D printing technique. It offers several advantages such as the absence of a post-printing processing, in
70 addition to its low-cost setup (Pereira et al. 2019; Sadia et al. 2018; Okwuosa et al. 2016). FDM 3D
71 printing involves the use of filaments, usually manufactured by hot melt extrusion (HME), as a pre-
72 product, which are then fed into the heated nozzle of the FDM 3D printer (Pereira et al. 2019; Sadia et
73 al. 2018; Okwuosa et al. 2016; Goyanes et al., 2014).

74 The potential of FDM 3D printing for on-demand manufacturing relies on producing stable,
75 reproducible, dose-consistent and ready-to-use filaments. In order to effectively utilise this technique,
76 these filaments should be easily mass-produced, packaged and stored before shipping to the printing
77 sites, including hospitals and community pharmacies. This will enable the vision of producing 3D
78 printed dosage forms that are intended to be dispensed shortly after being fabricated to match patients'
79 needs in small batches to be achieved, and should maintain at least the stability standards for
80 extemporaneous preparations. Therefore, the long-term stability of the filament, as a pre-product on the
81 shelves of manufacturing units or compounding pharmacies, is of paramount importance for the success
82 of this approach.

83 In the last six years, many studies have focused on the application of FDM 3D printing for dose
84 personalisation (Charoenying et al. 2020; Eleftheriadis et al. 2019; Jamróz et al. 2020; Wei et al. 2020;
85 Zhang et al. 2020; Fanous et al. 2020; Vo et al. 2020; Pereira et al. 2019; Sadia et al. 2018; Okwuosa et
86 al. 2016; Pietrzak et al. 2015). However, there are limited information about the long-term stability of
87 these filaments. In fact, changes in the physicochemical properties of the filament during storage might
88 not only compromise the efficacy of the active ingredient but may also affect its printability. Hence,
89 adding more complexity to the technical challenges (Ilyés et al. 2019). For instance, a reduced plasticity
90 of the filament upon storage will result in a brittle filament that may often break under pressure from
91 the FDM 3D printer head gears (Ilyés et al. 2019, Neserreddin et al., 2018). Moreover, other changes in
92 the filament diameter and/or shape may also have an impact on the final printed product, leading to
93 variations in 3D printed tablets weights (weight uniformity) and in some cases the failure to complete
94 the 3D printing process (Ilyés et al. 2019).

95 With many researchers working towards the adaptation of FDM 3D printing in pharmaceutical
96 manufacturing, there is the need to study the stability of commonly used pharmaceutical polymers
97 adapted to suit this novel manufacturing approach. In this work, the stability of HME-based filaments
98 at 5 °C or 30 °C + 65 %RH were investigated. The impacts of the storage and packaging conditions were
99 studied using theophylline as a model drug in combination with different model polymers. As the focus
100 of this work is the impact of storage condition on physical change and the printability of different
101 polymer-based filaments, a chemically stable molecule (Serajuddin, 1986), theophylline was selected
102 as a model drug. The filaments in this study have been previously investigated to achieve immediate
103 and modified release 3D printed structures using commercially available polymers of different chemical
104 nature and hygroscopicity [PVP-based (Okwuosa et al. 2016), HPS.SSL-based (Pietrzak et al. 2015),
105 L100-55-based, S100-based, RL-based and EPO-based filaments (Okwuosa et al. 2017; Sadia et al.
106 2018; Sadia et al. 2016)]. It is important to highlight that both Eudragit L100-55 and S100-based
107 filaments were used to fabricate the shell in delayed release system and hence were made drug-free.
108 The diameter, printability, thermal properties, physical form of the API, drug content of the filament,
109 and the drug release profile of the 3D printed dosage forms were investigated before and after exposure
110 to the storage conditions.

111

112 **2. Materials and Methods**

113 *2.1 Materials*

114 Hydroxypropyl cellulose (HPC.SSL) was obtained from Nisso Chemical Europe (Dusseldorf,
115 Germany). Theophylline was purchased from ACROS Organics. Polyvinylpyrrolidone (PVP,
116 MW 40,000), triacetin and triethyl citrate (TEC) were purchased from Sigma-Aldrich (UK). Talc was
117 purchased from Fluka Analytical (UK). Eudragit L100-55, RL, EPO and S100 were donated by Evonik
118 Industries (Darmstadt, Germany).
119

120 *2.2 Preparation of filaments*

121 The PVP, HPC SSL and Eudragit based filaments were produced by HME following previously
122 reported approach (Okwuosa et al. 2016). All filaments contained a model drug (theophylline) except
123 for Eudragit L100-55 and S100 based filaments, which were used to 3D print enteric layers (Okwuosa
124 et al. 2017). The composition, processing temperatures of the HME processes and nozzle sizes are
125 detailed in **Table 1**.
126

127 *2.3 Accelerated stability studies (storage conditions)*

128 In order to determine the stability of the filaments over a long-term storage, accelerated stability
129 studies were carried out according to the International Council for Harmonisation (ICH) guidelines
130 [Q1A(R2)] (ICH, 2003). The drug-loaded (PVP, HPC.SSL, Eudragit EPO and RL-based) and the drug-
131 free (Eudragit L100-55 and S100-based) filaments were sealed in polyvinyl chloride (PVC) polybags
132 with or without vacuuming and stored in a fridge at 5 °C or in an incubator at 30 °C + 65 %RH. Vacuum
133 sealing was achieved using Andrew James VS517 Dom Sealer. The filaments were characterised when
134 freshly prepared and then after 1, 3 and 6 months of storage.

135 *2.4 Filament dimension and visual appearance*

136 In order to determine the effect of the storage conditions on the diameter of the filaments,
137 changes in the diameter of the filaments were monitored using a Draper Electronic Digital caliper (0 –
138 25 mm) with a resolution of 0.01 mm. Filaments were observed to assess change in their visual
139 appearance (change in shape, colour or presence of aggregation).
140

141 *2.5 Printability test using FDM 3D printer*

142 The 3D printing of the filaments that were stored under different conditions was attempted
143 using the parameters detailed in **Table 1** to determine the effect of the storage conditions on 3D printing
144 in comparison to a freshly prepared filament using Makerbot Experimental 2X 3D printer (Makerbot
145 Inc, NY, USA). 3D Printing was carried out at a standard resolution (0.2 mm layer thickness) and a 100
146 % infill with rectilinear infill pattern. Other settings were set as previously detailed (Okwuosa et al.
147

148 2016). A caplet (L x W x H 10 x 4 x 3.6 mm) was designed and imported into the MakerWare software
149 Version 2.4.0.17 (Makerbot Industries, LLC., USA) and used to test the printability of the filaments.
150 The printed caplets weighed approximately 110 mg, containing approximately 11, 50, 50 and 52 mg of
151 theophylline for the PVP, HPC SSL, Eudragit RL and EPO-based caplets respectively.

152 2.6 *Thermal gravimetric analysis (TGA)*

153
154 TGA analysis for the extruded filaments was carried out using a TGA Q500 (TA Instruments,
155 Hertfordshire, UK). The filaments were cut into small pieces (<1mm, approximately 10 mg) were
156 accurately weighed and placed in a 40 μ L aluminium pan (TA Instruments, Hertfordshire, UK), which
157 was placed on a platinum pan. Samples were then scanned from 25 to 500 $^{\circ}$ C at a heating rate of 10
158 $^{\circ}$ C/min with a nitrogen purge of 40/60 mL/min for the sample and furnace, respectively. All
159 measurements were carried out in triplicates and the data analysed using a TA Universal Analysis 2000
160 software (TA Instruments, Hertfordshire, UK)

161 2.7 *Differential scanning calorimetry (DSC)*

162
163 For modulated temperature differential scanning calorimetry (MTDSC) analysis, a differential
164 scanning calorimeter (DSC) Q2000 (TA Instruments, Elstree, Hertfordshire, UK) was used. PVP-based
165 filaments were subjected to a modulated heat-cool-heat scan in order to measure and exclude the effect
166 of moisture content on the plasticity of the filaments. Eudragit L100-55 and S100-based filaments were
167 also subjected to a modulated scan. The modulation scan was applied using an amplitude of 0.212 $^{\circ}$ C
168 and a period of 40 sec, scanning from -70 to 200 $^{\circ}$ C at a heating rate of 2 $^{\circ}$ C/min.

169 As moisture did not interfere with the thermographs obtained unlike the aforementioned filaments, a
170 non-modulated standard scan was used for HPC SSL, Eudragit RL and EPO-based filaments from -50
171 to 200 $^{\circ}$ C at a heating rate of 10 $^{\circ}$ C/min. Analysis was carried out under a purge of nitrogen gas
172 (50 mL/min). All the data were analysed using a TA Universal Analysis 2000 software (TA
173 Instruments, Hertfordshire, UK). TA pin-holed standard lids and 40 μ L aluminium pans (TA
174 Instruments, Hertfordshire, UK) were filled with approximately 5 mg sample and sealed. All
175 measurements were carried out in triplicates.

176

177 2.8 *X-ray powder diffractometry (XRPD)*

178
179 X-ray powder diffraction was carried out on the filaments over 6 months to investigate changes
180 in the physical forms of the API or excipients. This was assessed using a powder X-ray diffractometer,
181 D2 Phaser with Lynxeye (Bruker, Germany). Filaments were dipped in liquid nitrogen before crushing
182 them using a mortar and pestle. The powders were scanned from 2Theta (2θ) = 5 $^{\circ}$ to 35 $^{\circ}$ using 0.01

183 step and 1.25 sec count. The divergence slit was 1 mm and the scatter slit 0.6 mm. The wavelength of
184 the X-ray was 0.154 nm using Cu source and a voltage of 30 kV and a current of 10 mA.

185 2.9 Determination of drug content (Eudragit EPO, RL, HPC.SSL and PVP-based filaments)

186
187 To determine changes in the drug contents of the filament after storage, 120 mg of the Eudragit
188 EPO and RL, HPC.SSL and PVP-based filaments containing theophylline were solubilised in 0.1 M
189 HCl and sonicated for 2h or 8 h (for Eudragit RL-based filament only). The API was measured by
190 HPLC using an Agilent UV-HPLC 1260 series (Agilent Technologies, Inc., Germany) and an XTerra
191 RP C18 column (150 × 4.6 mm, 5 µm particle size) (Waters, Ireland). A mobile phase of 10 mM solution
192 of ammonium acetate buffer, methanol and acetonitrile at volume ratio of 86:7:7. Analysis was carried
193 out at a wavelength of 272 nm, column temperature of 40 °C, flow rate of 1 mL/min, injection volume
194 was 5 µL and a run time of 7 min as reported previously (Okwuosa et al. 2016).

195 2.10 In vitro drug release studies (Eudragit EPO and RL-based filament)

196
197 In vitro drug release studies for the 3D printed tablets were carried out using a USP II
198 dissolution apparatus (AT 7 Smart, Sotax, Switzerland). The tablets were tested in 900 mL of 0.1 M
199 HCl solution for the EPO-based tablets for 2 hours. However, for the extended release formulation
200 (Eudragit RL), dissolution testing was carried out in 750 mL of HCl solution, followed by the addition
201 of 250 mL of 0.215 M tribasic phosphate buffer after 2hrs and the pH adjusted to 6.8. Samples were
202 collected for another 6 hrs. The samples were automatically collected and analysed at 5 min intervals
203 using a UV/VIS spectrophotometer (PG instruments limited, UK) at a wavelength of 272 nm. The path
204 length used was 1 mm. The data were analysed using IDIS Software version 3 Automated Lab
205 (Berkshire, UK).

206 2.11 Statistical analysis

207 One-way ANOVA was employed using SPSS Software (22.0.0.2) to analyse the results. the level
208 of statistical significance was set at ($p < 0.05$).

209

210 3. Results and discussions

211

212 The use of FDM 3D printing for on-demand dose personalisation relies greatly on the
213 manufacturing of stable filaments that will be able to withstand storage and transportation. This ensures
214 compatibility with the FDM 3D printer at the point of use, whilst maintaining the integrity of the loaded
215 APIs and meeting the individual needs of patients. Therefore, the goal of this research was to investigate
216 stability-related challenges that could be faced in the use of methacrylate, cellulose and polyvinyl
217 pyrrolidone-based filaments for FDM 3D printing.

218 3.1 Physical and thermal properties of the stored filaments

219 Changes in the physical and thermal properties of these filaments following storage could affect
220 their 3D printing into solid dosage forms. Therefore, the impact of the storage conditions on the
221 diameter of the filaments were investigated. It was observed that a filament diameter >1.8 mm will lead
222 to blockage due to its inability to pass through the liquifying chamber of the FDM 3D printer's head.
223 This is an essential quality criterion of the filaments to ensure consistent flow through the pressing gears
224 into the hot nozzle. In addition, deformations in the cylindrical shape of the filament (deviation from
225 the cylindrical shape) could potentially affect the filament interaction with the gears in the 3D printer,
226 leading to inconsistency of the flow through the hot nozzle. Such effect can result in weight variation
227 of the 3D printed product (data not included). These changes could also be influenced by the changes
228 in the thermal properties of the filaments, with the TGA analysis being able to investigate water gain or
229 loss and changes in the degradation profile of the stored filaments, with reference to the freshly prepared
230 samples. Also, changes in the glass transition temperature (T_g) of the filament can significantly alter
231 the mechanical properties of the filaments, in turn, the ability to load the filaments into the liquifying
232 chamber of the FDM 3D printer head. Therefore, investigations into the effect of the storage conditions
233 on the T_g of the filaments were also carried out using DSC.

234 a) *Methacrylate-based filaments*

235 Investigating the diameter of Eudragit EPO-based filaments after storage revealed that no change
236 was noted when stored at 5 °C. However, storing the filaments at 30 °C + 65 %RH resulted in a
237 permanent flattening/deformation of these filaments only when the storage bag was vacuum-sealed
238 (**Table 2, Supplementary Data Fig. S1**). The resultant deformation affected its compatibility with the
239 3D printer and prevented its conversion into a solid dosage form. The TGA analysis of this filament
240 demonstrated similar thermographs in the storage conditions (**Fig. 1A**) in comparison to a freshly
241 prepared sample with insignificant moisture uptake with no observed weight loss between 50-150 °C.
242 The non-hygroscopic nature of this polymer was also observed by Parikh et al. (2014), who recorded a
243 0.2 %w/w moisture content. On the other hand, the DSC analysis revealed a slight reduction in the T_g
244 of the filament due to storage (**Fig. 1B**). However, this did not affect the printability of the filaments

245 stored at 5 °C and 30 °C with no vacuuming. The flattening of the vacuum-sealed filament when stored
246 at 30 °C could be attributed to the increased mobility of the polymeric chains above the T_g of the
247 Eudragit EPO matrix. In addition, the negative pressure on the filaments due to the vacuuming, may
248 have contributed to the deformation of the filament. This was confirmed when a protective shell placed
249 around the filaments, resulted in no alteration in shape at the same storage conditions (data not
250 included).

251 The Eudragit RL-based filament also lost its original cylindrical shape when stored in a vacuumed
252 PVC bag at 30 °C and 65 % RH, and hence was incompatible with the FDM 3D printer only at this
253 storage condition (**Table 2**). This was also the case for Eudragit L100-55-based filaments. Both
254 Eudragit based filaments demonstrated no changes in their weight loss TGA patterns due to storage as
255 well as no indication of water uptake (**Figs. 2A and 3A**). The filaments stored at 5 °C (with or without
256 vacuuming) and in a non-vacuumed bag at 30 °C + 65% RH were easily printed, demonstrating desirable
257 filament properties. An increase in T_g was observed, however, this had no effect on the filament
258 printability (**Figs. 2B and 3B**) (Melocchi et al. 2020).

259 The dimensions of Eudragit S100-based filaments did not incur any significant changes due to
260 storage and maintained compatibility with the FDM 3D printer, irrespective of the storage condition
261 (**Table 2**). Their TGA thermographs remained similar during storage, demonstrating no water uptake
262 during the storage period (**Fig. 4A**). Unlike the previously discussed filaments, the S100-based
263 filaments demonstrated a higher T_g value (85-89 °C) (**Fig. 4B**), hence were unaffected by the storage
264 at 30 °C and the vacuuming pressure.

265 *b) Hydroxypropyl cellulose-based filaments*

266 The HPC-based filament deformed when stored in a vacuumed bag at 30 °C and 65% RH. In
267 addition, the filaments from other storage conditions were also incompatible with the FDM 3D printer.
268 The TGA analysis of the stored filaments showed weight gain values of 2.25 % and 2 %w/w for
269 filaments stored at 5 and 30 °C + 65% RH, respectively (**Fig. 5A**). This demonstrated the hygroscopic
270 nature of the cellulose-based matrix (Rowe et al. 2006). Water has often been reported to have a
271 plasticising effect on polymeric matrices (Teng et al. 2010), leading to a drop in the T_g of these
272 filaments from 36.7 to 34.9 °C after storage as demonstrated by DSC thermograph (**Fig. 5B**). This
273 confirms the potential role of water uptake as a major disruptor for compatibility with FDM 3D printing
274 process, due to increased flexibility. Such an increase will obstruct feeding into the liquifying chamber
275 of the FDM head, resulting in a poor grip of the gears on the filament and subsequently, the folding of
276 the filaments around the gears (Ilyés et al. 2019). This effect of high plasticity on the printability of the
277 filaments was also observed by Tan *et al.* (2020). As a result of these initial negative findings following
278 one-month storage, the HPC-based filaments were withdrawn from further studies.

279 *c) Povidone-based filaments*

280 Investigating the physical properties of the PVP-based filaments revealed their stability only at the
281 5 °C storage condition where they retained their shape and diameter. The TGA of freshly prepared PVP-
282 based filaments depicted an initial weight loss of approximately 4 % at around 120 °C due to moisture
283 loss, which could be attributed to the hygroscopic nature of PVP (Gupta et al. 2014). The storage of the
284 filaments at 5 °C resulted in up to 6.5 % water uptake (**Fig. 6**). PVP has been reported to be able to take
285 moisture up to 40% of its weight (Ramineni et al. 2013). It was not possible to determine precisely the
286 Tg of these filaments due to the excessive water evaporation upon heating, which interfered with the
287 detectability of the polymer's Tg. A heat-cool-heat DSC approach could eliminate these effects of
288 moisture. However, this approach led to the removal of moisture during the first heat scan and can mask
289 the potential of storage on Tg of the filament (**Supplementary Data, Figs. S2 and S3**). Such high
290 water-uptake was reported to produce a significant drop in its Tg (Fitzpatrick et al. 2002; Xie and Taylor
291 2017; Teng et al. 2010). Although the filaments at 5 °C remained compatible with the 3D printer, their
292 very hygroscopic nature poses a major challenge to their application. Therefore, a future product would
293 require the use a specific packaging for these filaments to provide moisture-controlled environment.
294 This might have major implications on the cost and practicality of using these filaments for on-demand
295 use in the community and hospital pharmacies.

296 **3.2 Impact of storage conditions on the physical form of theophylline**

297 Changes in the physical forms of theophylline and excipients due to storage can influence the
298 drug release profile. Due to the degradation of methacrylate polymers when thermally scanned >170 °C
299 (Parikh et al., 2016), it was not possible to use DSC to assess the physical form of theophylline (melting
300 point of 272.8 °C) (Kuzminska et al., 2021). To investigate this, XRPD was used to analyse the
301 filaments before and after storage. The Eudragit EPO, RL, HPC.SSL and PVP-based filaments loaded
302 with theophylline revealed the presence of diffraction peaks at $(2\theta) = 7$ and 12° (**Fig. 7**), which
303 correspond to theophylline crystals. Talc, which was used as the structure forming agent, demonstrated
304 sharp peaks at $(2\theta) = 9.52^\circ, 19.54^\circ, 28.87^\circ$. The intensity peaks indicated that a proportion of the API
305 remained crystalline within the filament, following thermal and mechanical stress of the HME processes
306 (Huang and Dai 2014). This proved to be dependent on the model APIs as previously investigated using
307 these matrices (Okwuosa et al. 2016; Sadia et al. 2016). The intensity peaks that corresponds to
308 theophylline were also observed after storage, indicating that a proportion of the API is in its crystalline
309 form during these storage conditions. However, the peak intensity at $(2\theta) = 12^\circ$ due to theophylline was
310 observed to increase for Eudragit EPO-based filament whilst it decreased for the Eudragit RL-based
311 filament over time (**Figs. 7A and B**). Variations in peak intensity has been linked to crystalline
312 concentrations (Siddiqui et al. 2015). Also, it was reported that partial crystalline nature of matrices
313 could alter due to storage (Lust et al. 2015; Huang and Dai 2014; Ueda et al. 2020). For filaments that

314 did not include drug (Eudragit L100-55 and S100), there were diffraction peaks at $(2\theta) = 9.52, 19.54,$
315 28.87 , which correspond to the crystals of talc, throughout the storage (**Supplementary Data, Figs. S4-**
316 **S7**).

317 **3.3 Drug integrity and *in vitro* drug release**

318 It was important that the integrity of the API-loaded in the filaments (Eudragit EPO, RL, HPC and
319 PVP-based) remains intact throughout the stability trial. This was important to ensure dosing accuracy
320 towards meeting the individual needs of patients using this novel manufacturing approach. HPLC
321 analysis showed no significant changes in API contents (**Supplementary Data, Table S1**), confirming
322 the stability of theophylline in the matrix.

323 Cellulose and the PVP-based filaments were deemed unstable and the L100-55 and S100-based
324 filaments were drug-free, therefore, the dissolution testing for the tablets printed from these filaments
325 was not investigated. *In vitro* release study on the PVP-based matrices demonstrated an increase in the
326 rate of drug release with the aging of the filament (**Fig. 8**), which was not as expected (Tian et al. 2014).
327 It is possible that the highly hygroscopic nature of PVP led to an increase in moisture contents within
328 the polymeric matrix. Drug mobility may also increase leading to phase separation and further drug
329 crystallisation (Chen et al. 2018).

330 Eudragit EPO is an immediate release polymer and as expected, the caplets from a freshly prepared
331 filament achieved more than 75 % theophylline release at 45 min. However, the rate of release slowed
332 down over time due to storage at 5 and 30 °C + 65 %RH (**Fig. 9**). This could be due to crystalline growth
333 during storage at high temperature and humidity (Tian et al. 2014). This was observed in the XRPD
334 analysis of the filament with peak intensity due to theophylline increasing as the filament ages. It is also
335 possible that during storage, polymer relaxation led to the formation of denser matrix, leading to reduced
336 dissolution rate. Phase separation was observed in a solid dispersion of indometacin and Eudragit EPO
337 produced by HME, which decreased the dissolution rate of the API (Sarode et al. 2013).

338 On the other hand, Eudragit RL-based tablets showed a faster drug release after storage at 5 °C in
339 comparison to the fresh sample (**Fig. 10**). A depression in peak intensity with aging was observed from
340 the XRPD studies, suggesting that more of the API became dissolved in the polymer over time.
341 Filaments stored at 30 °C did not show a significant change in drug release compared to a freshly
342 prepared product. A solid dispersion containing Eudragit RL and indometacin demonstrated no
343 alteration in drug release after exposure to 40 and 50 °C for a short period of time (5 h) (Azarmi et al.
344 2002).

345 In summary, the presented data suggested that filaments based on methacrylate polymers are less prone
346 to physical changes and remains compatible with FDM 3D printer following storage. Such findings are

347 particularly important to future efforts of engineering ‘a pharmaceutical ink’ based on HME drug-
348 loaded filaments to be used as a shelf-item for on demand manufacturing.

349 **4. Conclusions**

350

351 This work highlights some of the stability challenges facing HME based-filaments as a pre-product
352 shelf item for on-demand use via FDM 3D printing. Storage conditions had a major impact on the
353 physical properties of the filaments such as shape, dimensions, flexibility and hence compatibility with
354 the FDM 3D printing. In comparison to the cellulose- and povidone-based filaments, methacrylate-
355 based filaments (Eudragit EPO, RL, S100 and L100-55) were generally more physically stable and
356 continued to be printable following storage. Polymers of lower Tg required specific storage conditions
357 such as the use of a vacuumed container or fridge temperature. Filaments based on hygroscopic
358 polymers (HPC and PVP) were more sensitive to Tg alterations due to water uptake, leading to 3D
359 printing failures, and hence they were deemed less suitable to be used as a shelf-item product for on-
360 demand printing. Overall, the integrity of the API in the drug loaded filaments was maintained. This
361 research provides a pioneering preview on the long-term stability consideration of pharmaceutical
362 filaments. Further research is needed to confirm this trend with a wider range of polymers and to assess
363 the impact of filament storage on the compliance of 3D printed tablets with compendial criteria.

364 **References**

365

366 Al-Metwali, B., and H. Mulla. 2017. "Personalised dosing of medicines for children." *J Pharm*
367 *Pharmacol* 69 (5): 514-524. <https://doi.org/10.1111/jphp.12709>.

368 Azarmi, S., J. Farid, A. Nokhodchi, S. M. Bahari-Saravi, and H. Valizadeh. 2002. "Thermal treating as a
369 tool for sustained release of indomethacin from Eudragit RS and RL matrices." *International*
370 *Journal of Pharmaceutics* 246 (1): 171-177. [https://doi.org/https://doi.org/10.1016/S0378-5173\(02\)00378-2](https://doi.org/https://doi.org/10.1016/S0378-5173(02)00378-2).

372 Cella, Massimo, Catherijne Knibbe, Meindert Danhof, and Oscar Della Pasqua. 2010. "What is the right
373 dose for children?" *British journal of clinical pharmacology* 70 (4): 597-603.
374 <https://doi.org/10.1111/j.1365-2125.2009.03591.x>.

375 Charoenying, Thapakorn, Prasopchai Patrojanasophon, Tanasait Ngawhirunpat, Theerasak
376 Rojanarata, Prasert Akkaramongkolporn, and Praneet Opanasopit. 2020. "Three-dimensional
377 (3D)-printed devices composed of hydrophilic cap and hydrophobic body for improving
378 buoyancy and gastric retention of domperidone tablets." *European Journal of Pharmaceutical*
379 *Sciences* 155: 105555. <https://doi.org/https://doi.org/10.1016/j.ejps.2020.105555>.

380 Chen, Huijun, Yipshu Pui, Chengyu Liu, Zhen Chen, Ching-Chiang Su, Michael Hageman, Munir Hussain,
381 Roy Haskell, Kevin Stefanski, Kimberly Foster, Olafur Gudmundsson, and Feng Qian. 2018.
382 "Moisture-Induced Amorphous Phase Separation of Amorphous Solid Dispersions: Molecular
383 Mechanism, Microstructure, and Its Impact on Dissolution Performance." *Journal of*
384 *Pharmaceutical Sciences* 107 (1): 317-326.
385 <https://doi.org/https://doi.org/10.1016/j.xphs.2017.10.028>.

386 Eleftheriadis, Georgios K., Christos Ritzoulis, Nikolaos Bouropoulos, Dimitrios Tzetzis, Dimitrios A.
387 Andreadis, Johan Boetker, Jukka Rantanen, and Dimitrios G. Fatouros. 2019. "Unidirectional
388 drug release from 3D printed mucoadhesive buccal films using FDM technology: In vitro and
389 ex vivo evaluation." *European Journal of Pharmaceutics and Biopharmaceutics* 144: 180-192.
390 <https://doi.org/https://doi.org/10.1016/j.ejpb.2019.09.018>.

391 Fanous, Marina, Sarah Gold, Stefan Hirsch, Joerg Ogorka, and Georgios Imanidis. 2020. "Development
392 of immediate release (IR) 3D-printed oral dosage forms with focus on industrial relevance."
393 *European Journal of Pharmaceutical Sciences* 155: 105558.
394 <https://doi.org/https://doi.org/10.1016/j.ejps.2020.105558>.

395 Fitzpatrick, Shaun, James F. McCabe, Catherine R. Petts, and Steven W. Booth. 2002. "Effect of
396 moisture on polyvinylpyrrolidone in accelerated stability testing." *International Journal of*
397 *Pharmaceutics* 246 (1): 143-151. [https://doi.org/https://doi.org/10.1016/S0378-5173\(02\)00375-7](https://doi.org/https://doi.org/10.1016/S0378-5173(02)00375-7). <http://www.sciencedirect.com/science/article/pii/S0378517302003757>.

399 Goyanes, A., Buanz, A.B., Basit, A.W., Gaisford, S., 2014. Fused-filament 3D printing (3DP) for
400 fabrication of tablets. *International journal of pharmaceutics* 476, 88-92.

401

402 Gupta, Simerdeep Singh, Anuprabha Meena, Tapan Parikh, and Abu T.M. Serajuddin. 2014.
403 *Investigation of thermal and viscoelastic properties of polymers relevant to hot melt extrusion*
404 *- I: Polyvinylpyrrolidone and related polymers*. Vol. 5.

405 Habib, W. A., A. S. Alanizi, M. M. Abdelhamid, and F. K. Alanizi. 2014. "Accuracy of tablet splitting:
406 Comparison study between hand splitting and tablet cutter." *Saudi Pharm J* 22 (5): 454-9.
407 <https://doi.org/10.1016/j.jsps.2013.12.014>.

408 Huang, Yanbin, and Wei-Guo Dai. 2014. "Fundamental aspects of solid dispersion technology for
409 poorly soluble drugs." *Acta Pharmaceutica Sinica B* 4 (1): 18-25.
410 <https://doi.org/https://doi.org/10.1016/j.apsb.2013.11.001>.

411 Ilyés, Kinga, Norbert Krisztián Kovács, Attila Balogh, Enikő Borbás, Balázs Farkas, Tibor Casian, György
412 Marosi, Ioan Tomuță, and Zsombor Kristóf Nagy. 2019. "The applicability of pharmaceutical
413 polymeric blends for the fused deposition modelling (FDM) 3D technique: Material
414 considerations—printability—process modulation, with consecutive effects on in vitro release,

415 stability and degradation." *European Journal of Pharmaceutical Sciences* 129: 110-123.
416 <https://doi.org/https://doi.org/10.1016/j.ejps.2018.12.019>.

417 ICH Harmonised Tripartite Guideline. 2003. "Stability Testing of New Drug Substances and Products
418 Q1A(R2)." Accessed
419 31/12. <https://database.ich.org/sites/default/files/Q1A%28R2%29%20Guideline.pdf>.

420 Isreb, A., K. Baj, M. Wojsz, M. Isreb, M. Peak, and M. A. Alhnan. 2019. "3D printed oral theophylline
421 doses with innovative 'radiator-like' design: Impact of polyethylene oxide (PEO) molecular
422 weight." *Int J Pharm* 564: 98-105. <https://doi.org/10.1016/j.ijpharm.2019.04.017>.

423 Jamróz, Witold, Mateusz Kurek, Joanna Szafranec-Szczęsny, Anna Czech, Karolina Gawlak, Justyna
424 Knapik-Kowalczyk, Bartosz Leszczyński, Andrzej Wróbel, Marian Paluch, and Renata
425 Jachowicz. 2020. "Speed it up, slow it down...An issue of bicalutamide release from 3D printed
426 tablets." *European Journal of Pharmaceutical Sciences* 143: 105169.
427 <https://doi.org/https://doi.org/10.1016/j.ejps.2019.105169>.

428 Kuzminska, M., Pereira, B.C., Habashy, R., Peak, M., Isreb, M., Gough, T.D., Isreb, A., Alhnan, M.A.,
429 2021. Solvent-free Temperature-Facilitated Direct Extrusion 3D Printing for Pharmaceuticals.
430 *International journal of pharmaceutics*, 120305.

431 Lust, Andres, Clare J. Strachan, Peep Veski, Jaakko Aaltonen, Jyrki Heinämäki, Jouko Yliruusi, and Karin
432 Kogermann. 2015. "Amorphous solid dispersions of piroxicam and Soluplus®: Qualitative and
433 quantitative analysis of piroxicam recrystallization during storage." *International Journal of*
434 *Pharmaceutics* 486 (1): 306-314.
435 <https://doi.org/https://doi.org/10.1016/j.ijpharm.2015.03.079>.

436 Martinez, P. R., A. Goyanes, A. W. Basit, and S. Gaisford. 2018. "Influence of Geometry on the Drug
437 Release Profiles of Stereolithographic (SLA) 3D-Printed Tablets." *AAPS PharmSciTech* 19 (8):
438 3355-3361. <https://doi.org/10.1208/s12249-018-1075-3>.

439 Melocchi, Alice, Marco Ubaldi, Alessandra Maroni, Anastasia Foppoli, Luca Palugan, Lucia Zema, and
440 Andrea Gazzaniga. 2020. "3D printing by fused deposition modeling of single- and multi-
441 compartment hollow systems for oral delivery – A review." *International Journal of*
442 *Pharmaceutics* 579: 119155. <https://doi.org/https://doi.org/10.1016/j.ijpharm.2020.119155>.

443 Nasereddin, J.M., Wellner, N., Alhijaj, M., Belton, P., Qi, S., 2018. Development of a Simple
444 Mechanical Screening Method for Predicting the Feedability of a Pharmaceutical FDM 3D
445 Printing Filament. *Pharm Res* 35, 151.

446 Nyboe Andersen, A., S. M. Nelson, B. C. Fauser, J. A. García-Velasco, B. M. Klein, and J. C. Arce. 2017.
447 "Individualized versus conventional ovarian stimulation for in vitro fertilization: a multicenter,
448 randomized, controlled, assessor-blinded, phase 3 noninferiority trial." *Fertil Steril* 107 (2):
449 387-396.e4. <https://doi.org/10.1016/j.fertnstert.2016.10.033>.

450 Okwuosa, T.C., Pereira, B.C., Arafat, B., Cieszyńska, M., Isreb, A., Alhnan, M.A., 2017. Fabricating a
451 Shell-Core Delayed Release Tablet Using Dual FDM 3D Printing for Patient-Centred Therapy.
452 *Pharm Res* 34, 427-437.

453 Okwuosa, Tochukwu C., Dominika Stefaniak, Basel Arafat, Abdullah Isreb, Ka-Wai Wan, and Mohamed
454 A. Alhnan. 2016. "A Lower Temperature FDM 3D Printing for the Manufacture of Patient-
455 Specific Immediate Release Tablets." *Pharmaceutical Research* 33 (11): 2704-2712.
456 <https://doi.org/10.1007/s11095-016-1995-0>. <http://dx.doi.org/10.1007/s11095-016-1995-0>.

457 Parikh, Tapan, Simerdeep Singh Gupta, Anuprabha Meena, and Abu Serajuddin. 2014. "Investigation
458 of thermal and viscoelastic properties of polymers relevant to hot melt extrusion - III:
459 Polymethacrylates and polymethacrylic acid based polymers." *Journal of Excipients and Food*
460 *Chemicals* 5: 56-64.

461 Patel, J. N., B. H. O'Neil, A. M. Deal, J. G. Ibrahim, G. B. Sherrill, O. A. Olajide, P. M. Atluri, J. J. Inzerillo,
462 C. H. Chay, H. L. McLeod, and C. M. Walko. 2014. "A community-based multicenter trial of
463 pharmacokinetically guided 5-fluorouracil dosing for personalized colorectal cancer therapy."
464 *Oncologist* 19 (9): 959-65. <https://doi.org/10.1634/theoncologist.2014-0132>.

465 Pereira, B. C., A. Isreb, R. T. Forbes, F. Dores, R. Habashy, J. B. Petit, M. A. Alhnan, and E. F. Oga. 2019.
466 "Temporary Plasticiser": A novel solution to fabricate 3D printed patient-centred
467 cardiovascular 'Polypill' architectures." *Eur J Pharm Biopharm* 135: 94-103.
468 <https://doi.org/10.1016/j.ejpb.2018.12.009>.

469 Pietrzak, K., A. Isreb, and M. A. Alhnan. 2015. "A flexible-dose dispenser for immediate and extended
470 release 3D printed tablets." *Eur J Pharm Biopharm* 96: 380-7.
471 <https://doi.org/10.1016/j.ejpb.2015.07.027>.

472 Ramineni, Sandeep K., Larry L. Cunningham, Thomas D. Dziubla, and David A. Puleo. 2013.
473 "COMPETING PROPERTIES OF MUCOADHESIVE FILMS DESIGNED FOR LOCALIZED DELIVERY OF
474 IMIQUIMOD." *Biomaterials science* 1 (7): 753-762. <https://doi.org/10.1039/C3BM60064E>.

475 Rowe, Raymond C., Paul J. Sheskey, and Siân C. Owen. 2006. *Handbook of pharmaceutical excipients*.
476 5th ed. Vol. Book, Whole. London: Pharmaceutical Press.

477 Sadia, M., A. Isreb, I. Abbadi, M. Isreb, D. Aziz, A. Selo, P. Timmins, and M. A. Alhnan. 2018. "From
478 'fixed dose combinations' to 'a dynamic dose combiner': 3D printed bi-layer antihypertensive
479 tablets." *Eur J Pharm Sci* 123: 484-494. <https://doi.org/10.1016/j.ejps.2018.07.045>.

480 Sadia, M., A. Sosnicka, B. Arafat, A. Isreb, W. Ahmed, A. Kelarakis, and M. A. Alhnan. 2016. "Adaptation
481 of pharmaceutical excipients to FDM 3D printing for the fabrication of patient-tailored
482 immediate release tablets." *Int J Pharm* 513 (1-2): 659-668.
483 <https://doi.org/10.1016/j.ijpharm.2016.09.050>.

484 Sarode, Ashish L., Harpreet Sandhu, Navnit Shah, Waseem Malick, and Hossein Zia. 2013. "Hot Melt
485 Extrusion for Amorphous Solid Dispersions: Temperature and Moisture Activated Drug-
486 Polymer Interactions for Enhanced Stability." *Molecular Pharmaceutics* 10 (10): 3665-3675.
487 <https://doi.org/10.1021/mp400165b>. <https://doi.org/10.1021/mp400165b>.

488 Sen, Koyel, Arushi Manchanda, Tanu Mehta, Anson W. K. Ma, and Bodhisattwa Chaudhuri. 2020.
489 "Formulation design for inkjet-based 3D printed tablets." *International Journal of*
490 *Pharmaceutics* 584: 119430. <https://doi.org/https://doi.org/10.1016/j.ijpharm.2020.119430>.

491 Serajuddin, A.T., 1986. Comparative thermal properties of the monohydrates of sodium theophylline
492 and theophylline. *J Pharm Pharmacol* 38, 93-96.

493 Siddiqui, A., Z. Rahman, M. Korang-Yeboah, and M. A. Khan. 2015. "Development and validation of X-
494 ray diffraction method for quantitative determination of crystallinity in warfarin sodium
495 products." *Int J Pharm* 493 (1-2): 1-6. <https://doi.org/10.1016/j.ijpharm.2015.07.051>.

496 Tagami, T., M. Ando, N. Nagata, E. Goto, N. Yoshimura, T. Takeuchi, T. Noda, and T. Ozeki. 2019.
497 "Fabrication of Naftopidil-Loaded Tablets Using a Semisolid Extrusion-Type 3D Printer and the
498 Characteristics of the Printed Hydrogel and Resulting Tablets." *J Pharm Sci* 108 (2): 907-913.
499 <https://doi.org/10.1016/j.xphs.2018.08.026>.

500 Tan, D. K., M. Maniruzzaman, and A. Nokhodchi. 2020. "Development and Optimisation of Novel
501 Polymeric Compositions for Sustained Release Theophylline Caplets (PrintCap) via FDM 3D
502 Printing." *Polymers (Basel)* 12 (1). <https://doi.org/10.3390/polym12010027>.

503 Teng, Jing, Simon Bates, David A. Engers, Kevin Leach, Paul Schields, and Yonglai Yang. 2010. "Effect
504 of Water Vapor Sorption on Local Structure of Poly(vinylpyrrolidone)." *Journal of*
505 *Pharmaceutical Sciences* 99 (9): 3815-3825.
506 <https://doi.org/https://doi.org/10.1002/jps.22204>.

507 Tian, Bin, Ling Zhang, Zhendong Pan, Jingxin Gou, Yu Zhang, and Xing Tang. 2014. "A comparison of
508 the effect of temperature and moisture on the solid dispersions: Aging and crystallization."
509 *International Journal of Pharmaceutics* 475 (1): 385-392.
510 <https://doi.org/https://doi.org/10.1016/j.ijpharm.2014.09.010>.

511 Ueda, Keisuke, Hitomi Okada, Zhijing Zhao, Kenjiro Higashi, and Kunikazu Moribe. 2020. "Application
512 of solid-state ¹³C relaxation time to prediction of the recrystallization inhibition strength of
513 polymers on amorphous felodipine at low polymer loading." *International Journal of*
514 *Pharmaceutics* 581: 119300. <https://doi.org/https://doi.org/10.1016/j.ijpharm.2020.119300>.

515 Vo, Anh Q., Jiaxiang Zhang, Dinesh Nyavanandi, Suresh Bandari, and Michael A. Repka. 2020. "Hot melt
516 extrusion paired fused deposition modeling 3D printing to develop hydroxypropyl cellulose
517 based floating tablets of cinnarizine." *Carbohydrate Polymers* 246: 116519.
518 <https://doi.org/https://doi.org/10.1016/j.carbpol.2020.116519>.

519 Wei, Can, Nayan G. Solanki, Jaydip M. Vasoya, Ankita V. Shah, and Abu T. M. Serajuddin. 2020.
520 "Development of 3D Printed Tablets by Fused Deposition Modeling Using Polyvinyl Alcohol as
521 Polymeric Matrix for Rapid Drug Release." *Journal of Pharmaceutical Sciences* 109 (4): 1558-
522 1572. <https://doi.org/https://doi.org/10.1016/j.xphs.2020.01.015>.

523 Xie, Tian, and Lynne S. Taylor. 2017. "Effect of Temperature and Moisture on the Physical Stability of
524 Binary and Ternary Amorphous Solid Dispersions of Celecoxib." *Journal of Pharmaceutical
525 Sciences* 106 (1): 100-110. <https://doi.org/https://doi.org/10.1016/j.xphs.2016.06.017>.

526 Zhang, Jiayang, Rishi Thakkar, Yu Zhang, and Mohammed Maniruzzaman. 2020. "Structure-Function
527 Correlation and Personalized 3D Printed Tablets using a Quality by Design (QbD) Approach."
528 *International Journal of Pharmaceutics*: 119945.
529 <https://doi.org/https://doi.org/10.1016/j.ijpharm.2020.119945>.

530

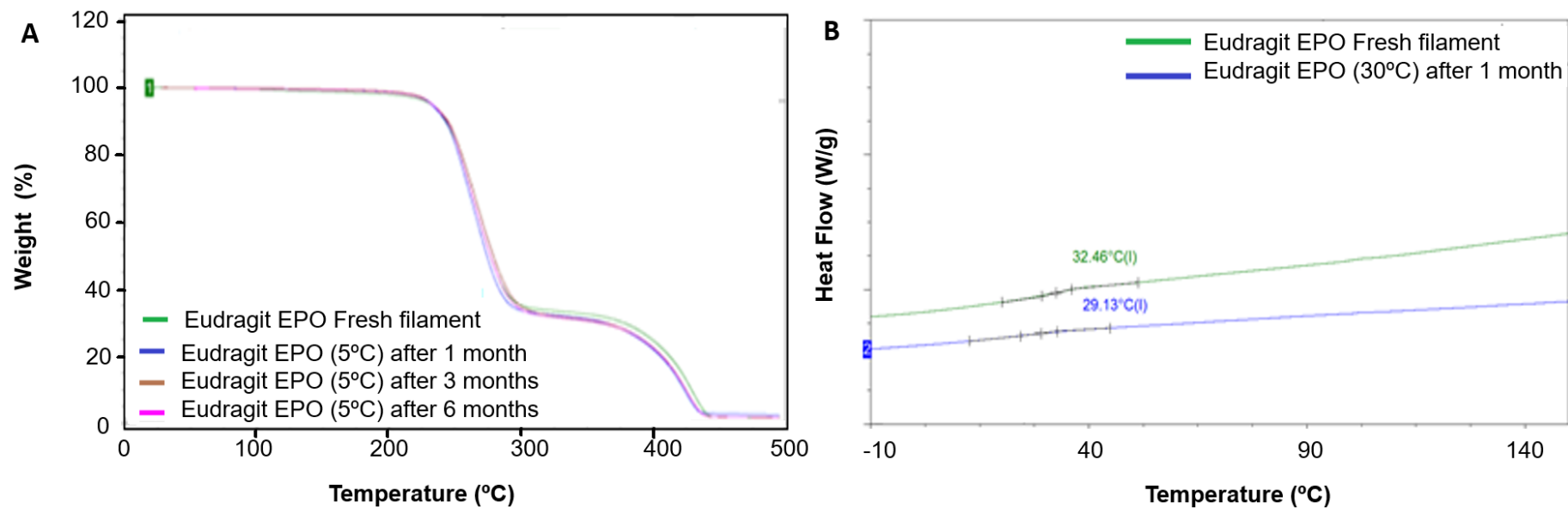


Fig. 1. (A) TGA thermographs for the impact of the storage condition (5 °C) on Eudragit EPO-based filament, (B) DSC thermographs for the impact of the storage condition (30 °C+ 65% RH+ vacuum) on Eudragit EPO-based filament (filaments deformed and no further assessment was carried out after 1 month).

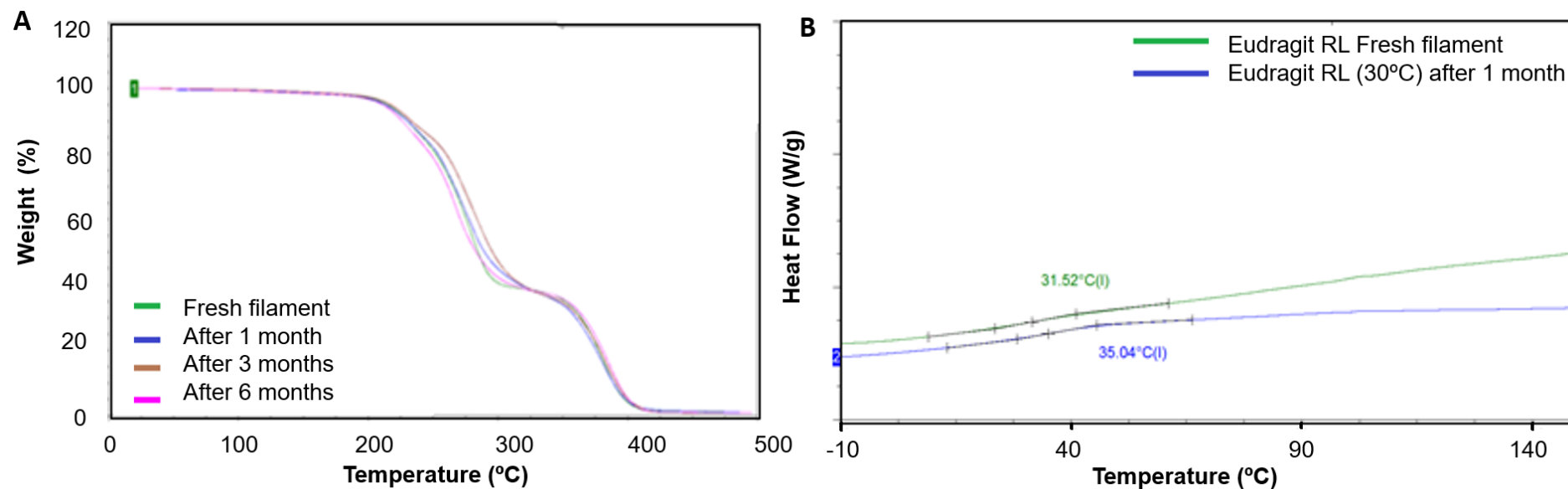


Fig. 2. TGA (A) thermographs for the impact of the storage condition (30 °C + vacuum) on Eudragit RL-based filament, (B) DSC thermographs for the impact of the storage condition (30 °C+ 65% RH+ vacuum) on Eudragit RL-based filament (filaments deformed and no further assessment was carried out after 1 month).

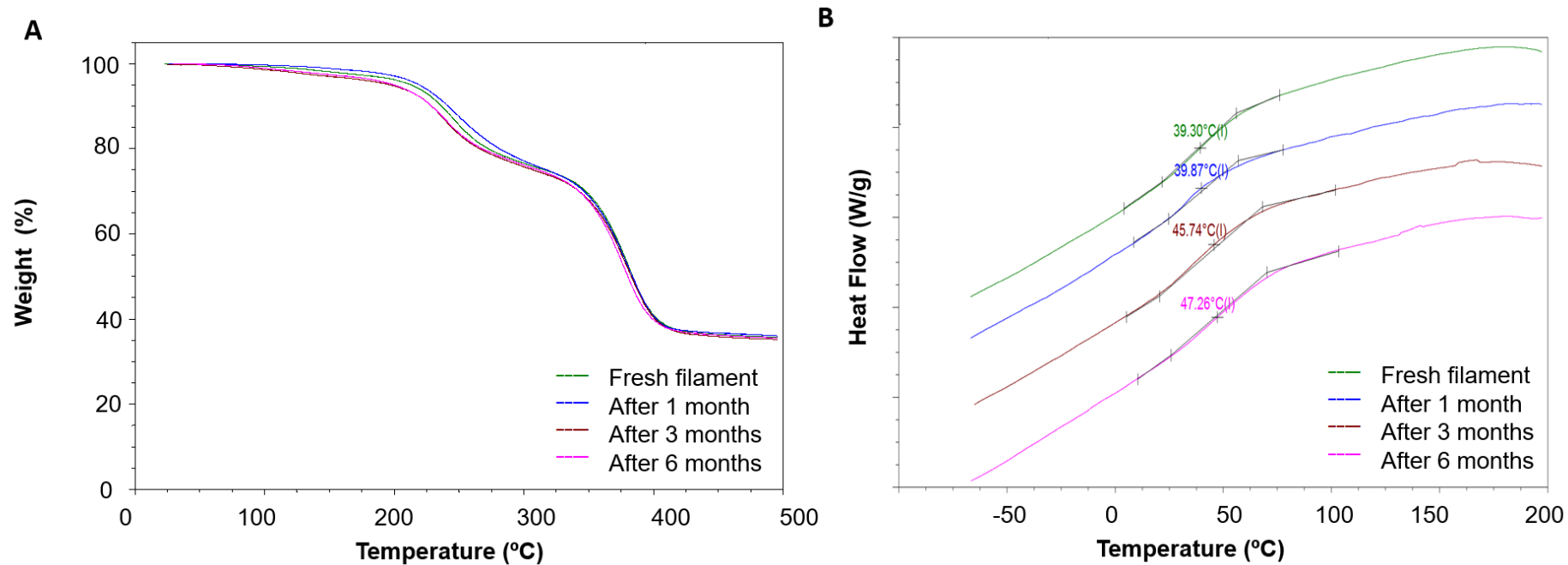


Fig. 3. TGA (A) and DSC (B) thermographs for the impact of the storage conditions (30 °C + 65% RH + vaccum) on the Eudragit L100-55-based filaments.

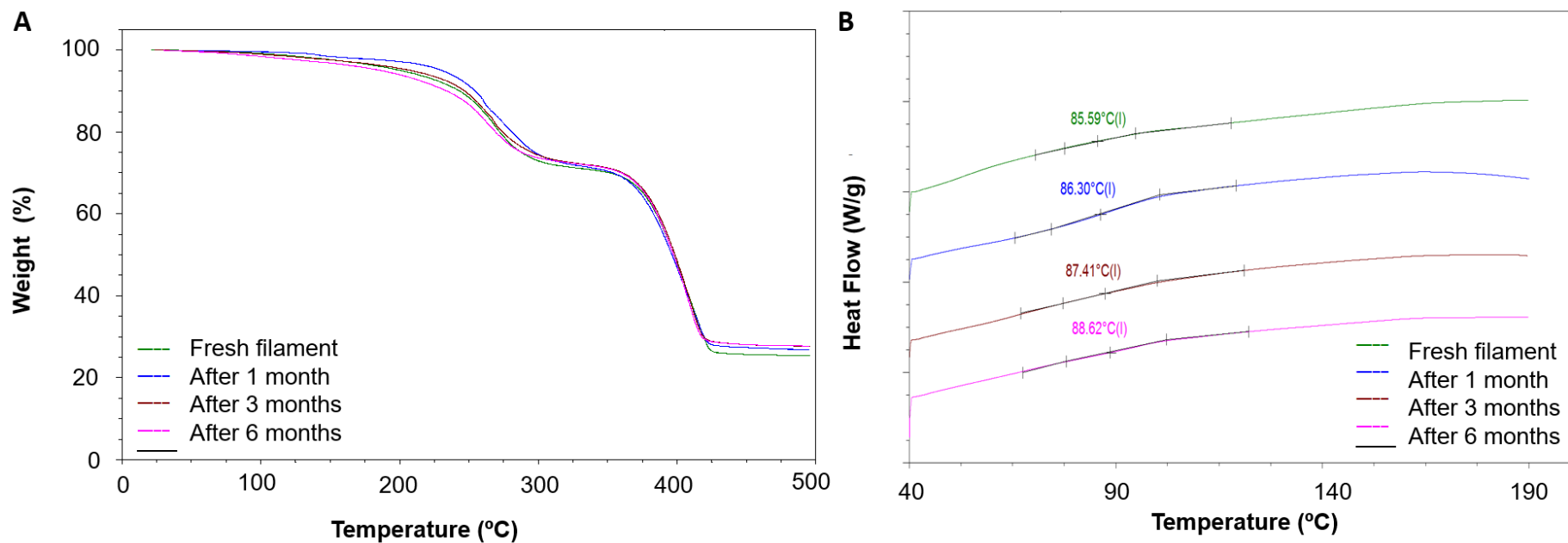


Fig. 4. Representative TGA (A) and DSC (B) thermographs for the impact of the storage conditions (30 °C + 65% RH + Vac) on the Eudragit S100-based filaments.

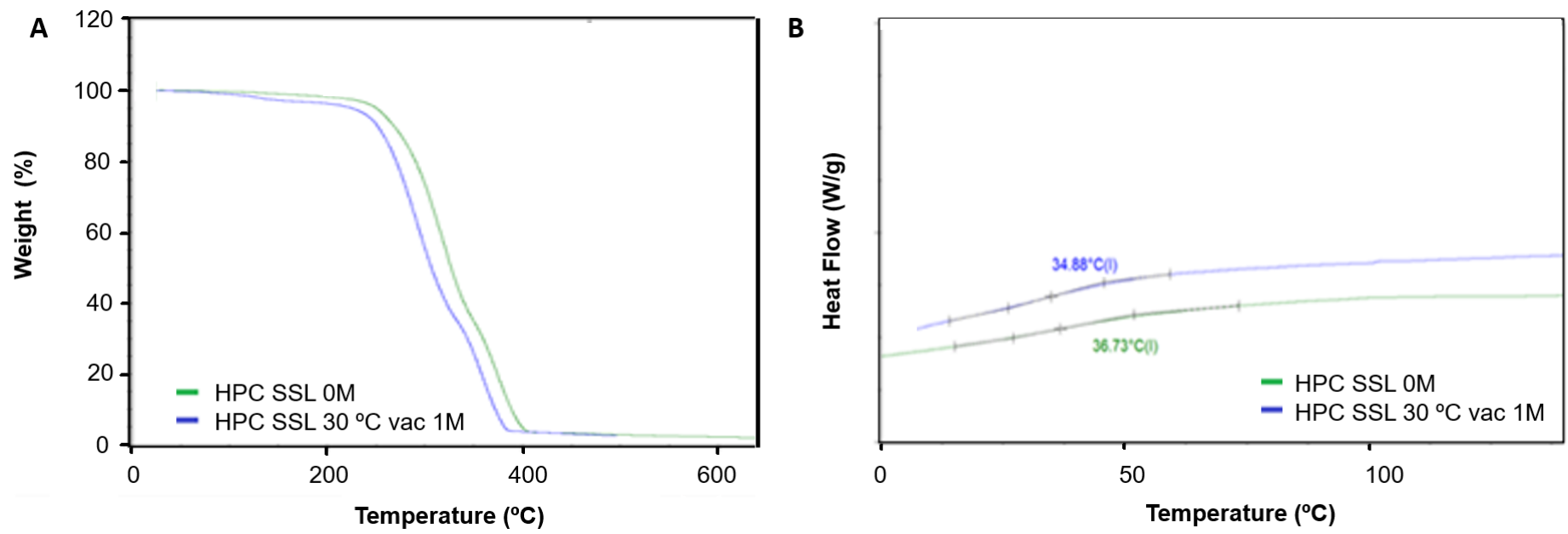


Fig. 5. TGA (A) and DSC (B) thermographs for the impact of the storage conditions on the HPC.SSL-based filaments.

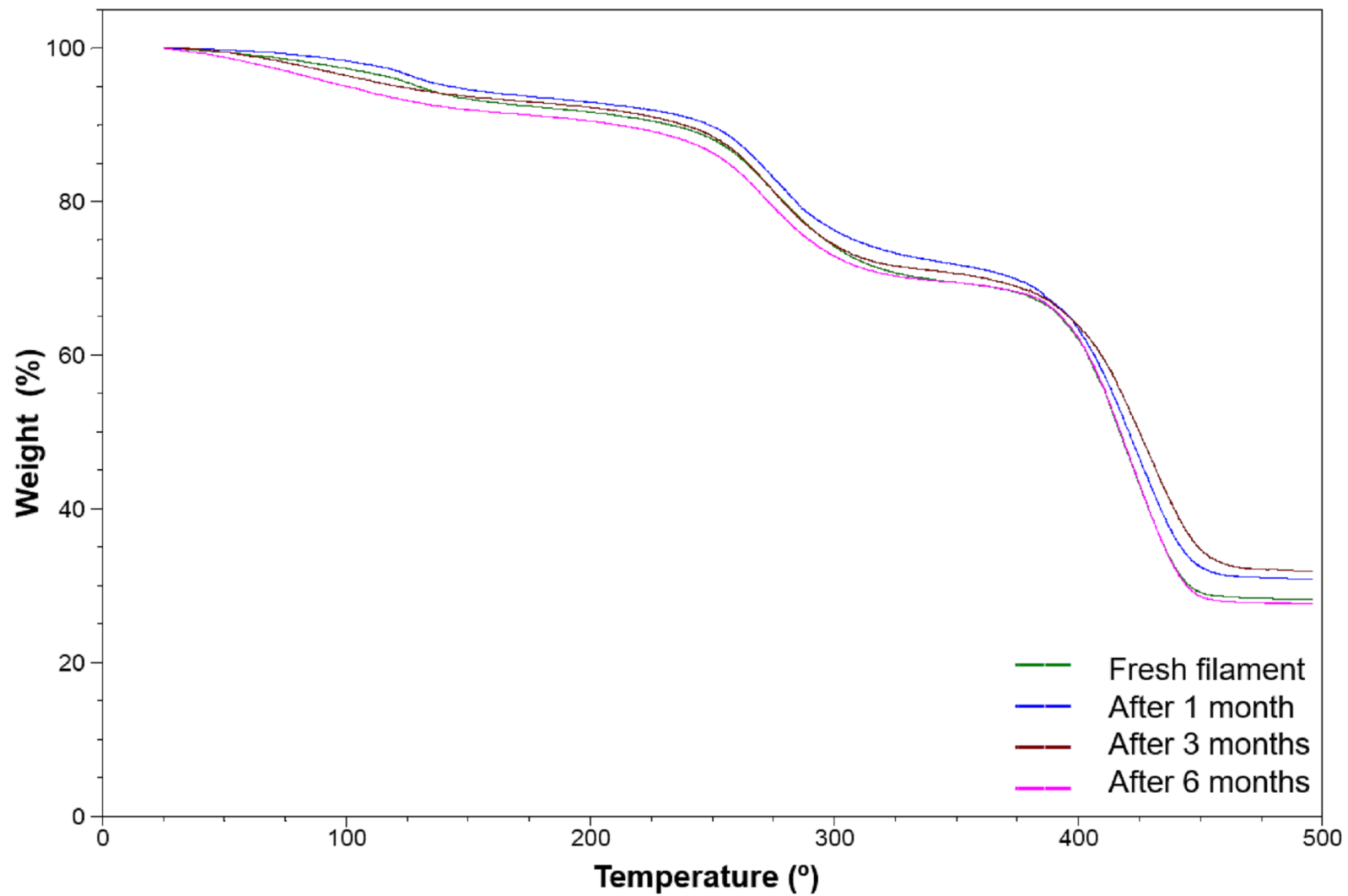


Fig. 6. TGA thermographs for the impact of the storage conditions (5 °C) on the PVP-based filaments.

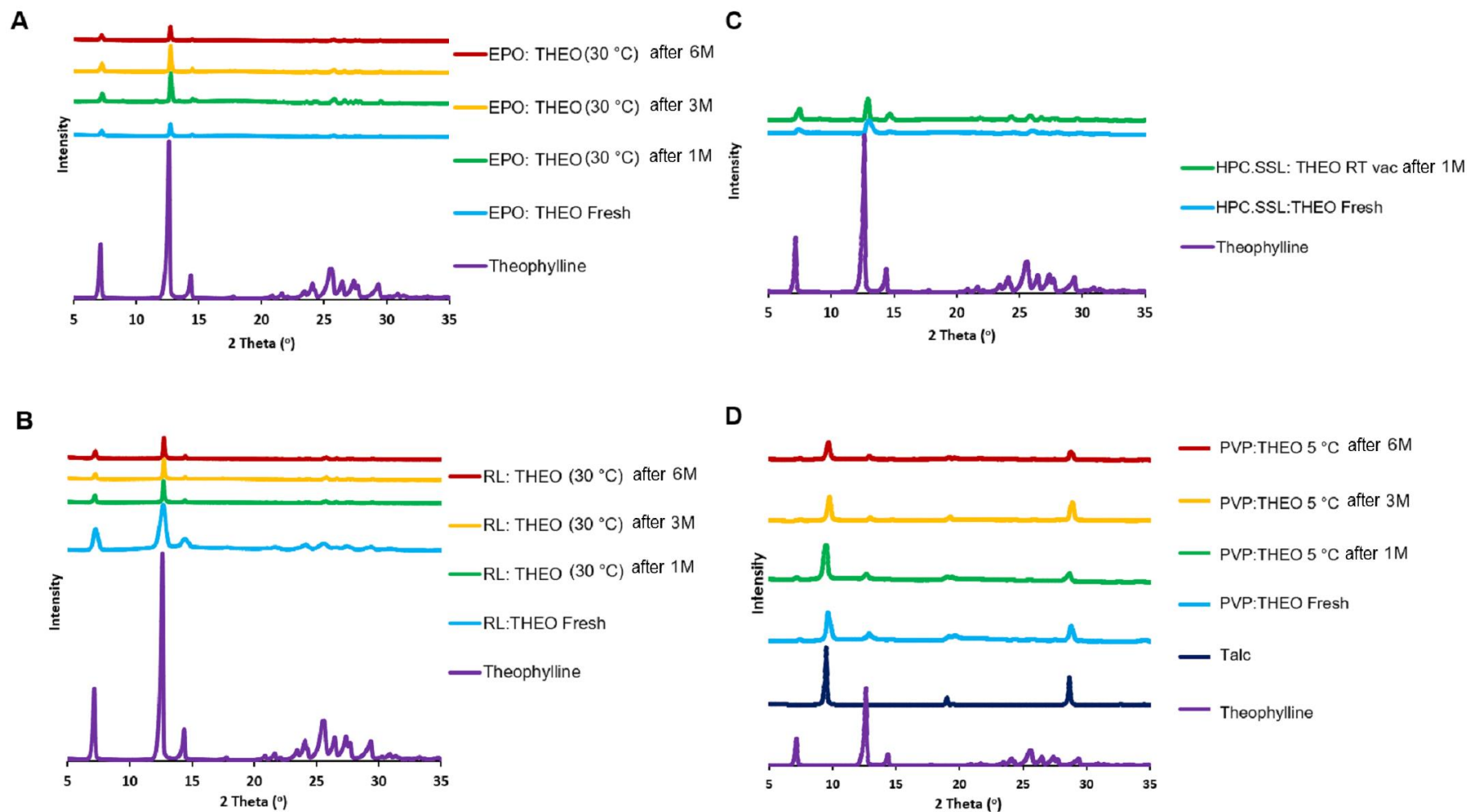


Fig. 7. XRPD data for the impact of the storage conditions on the Eudragit EPO (A), Eudragit RL (B), HPC.SSL (C) and PVP (D)-based drug loaded filament

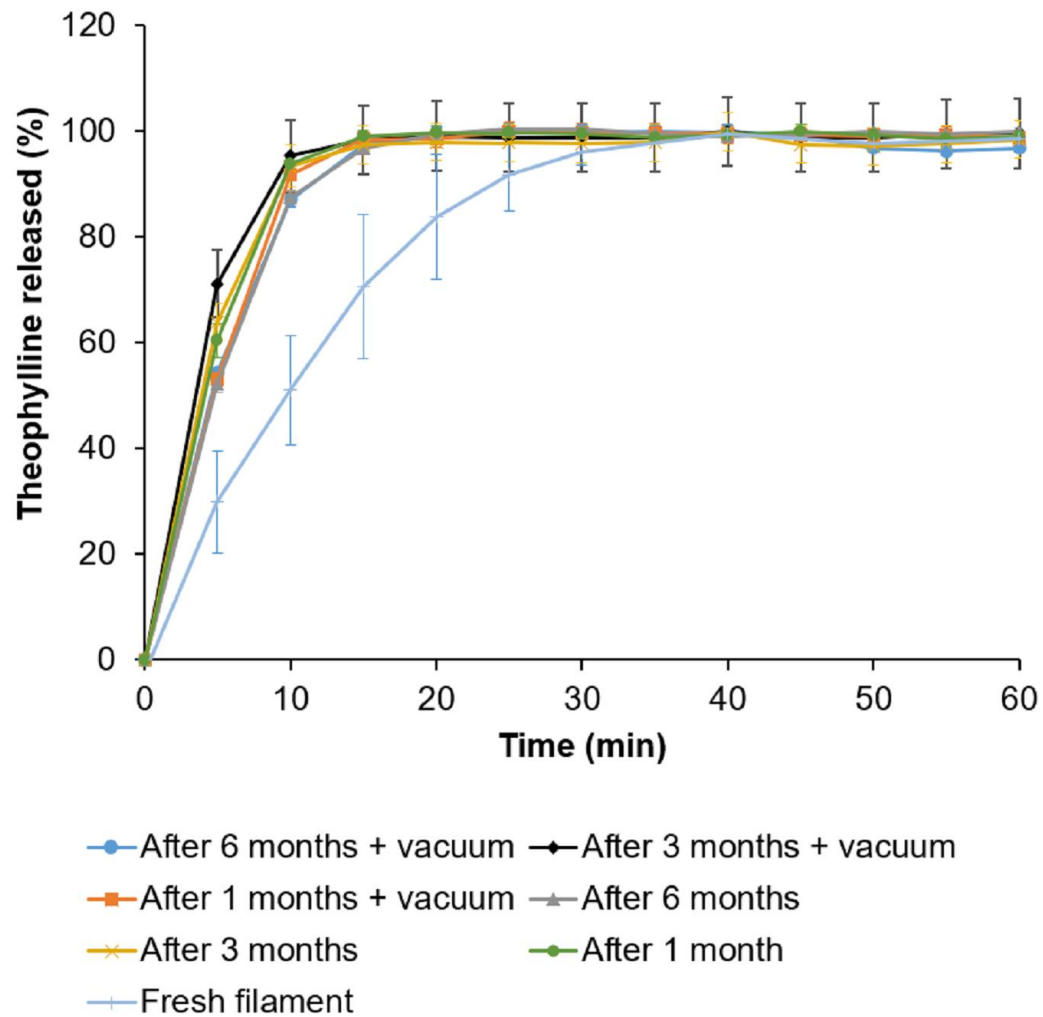


Fig. 8. The impact of storage at 5 °C on the *in-vitro* release profile of theophylline from the PVP-based product.

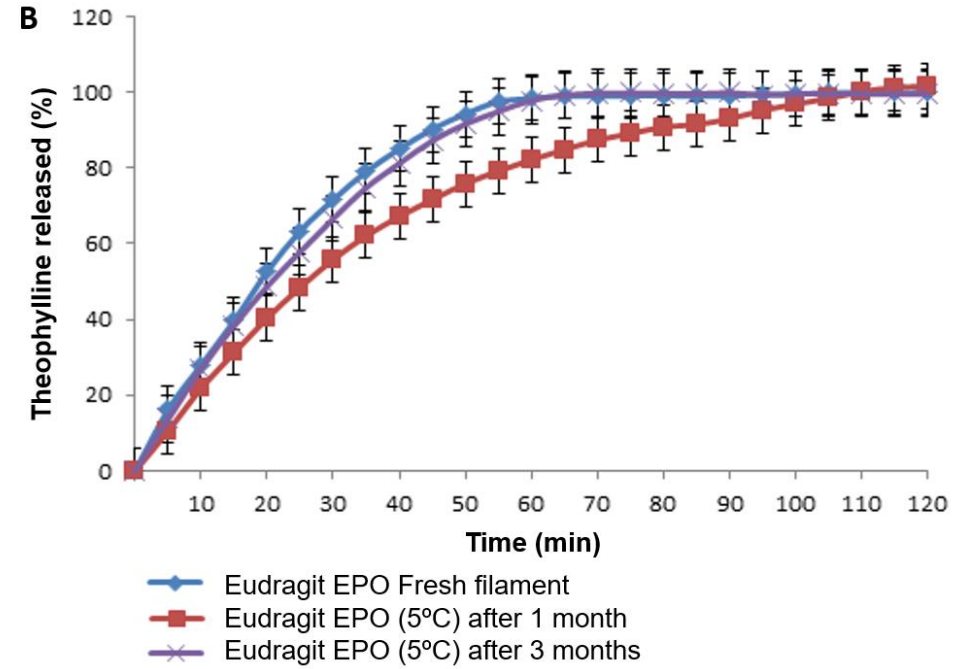
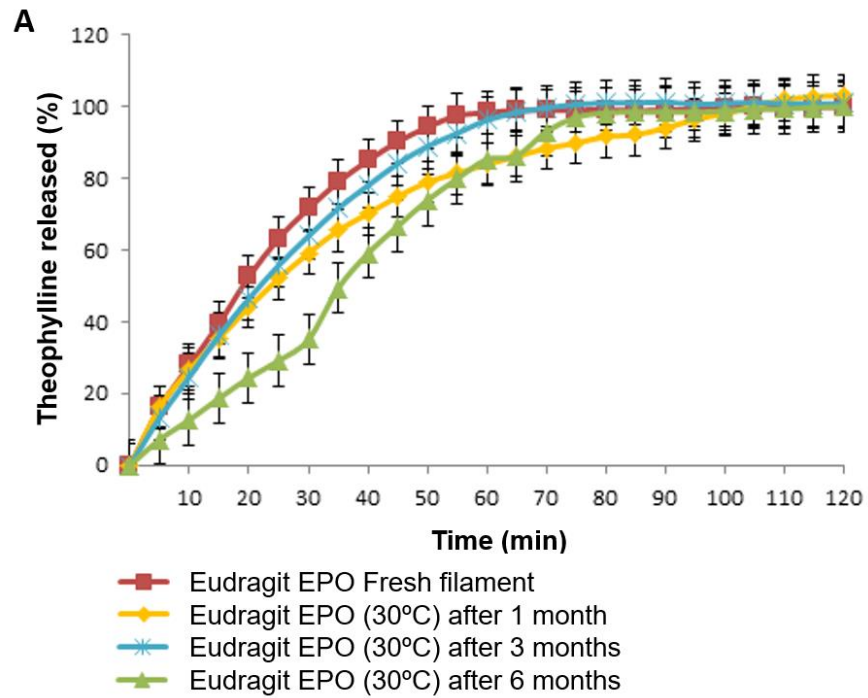


Fig. 9. The impact of the storage conditions on the *in-vitro* drug release profile of theophylline from the Eudragit EPO-based 3D printed tablets.

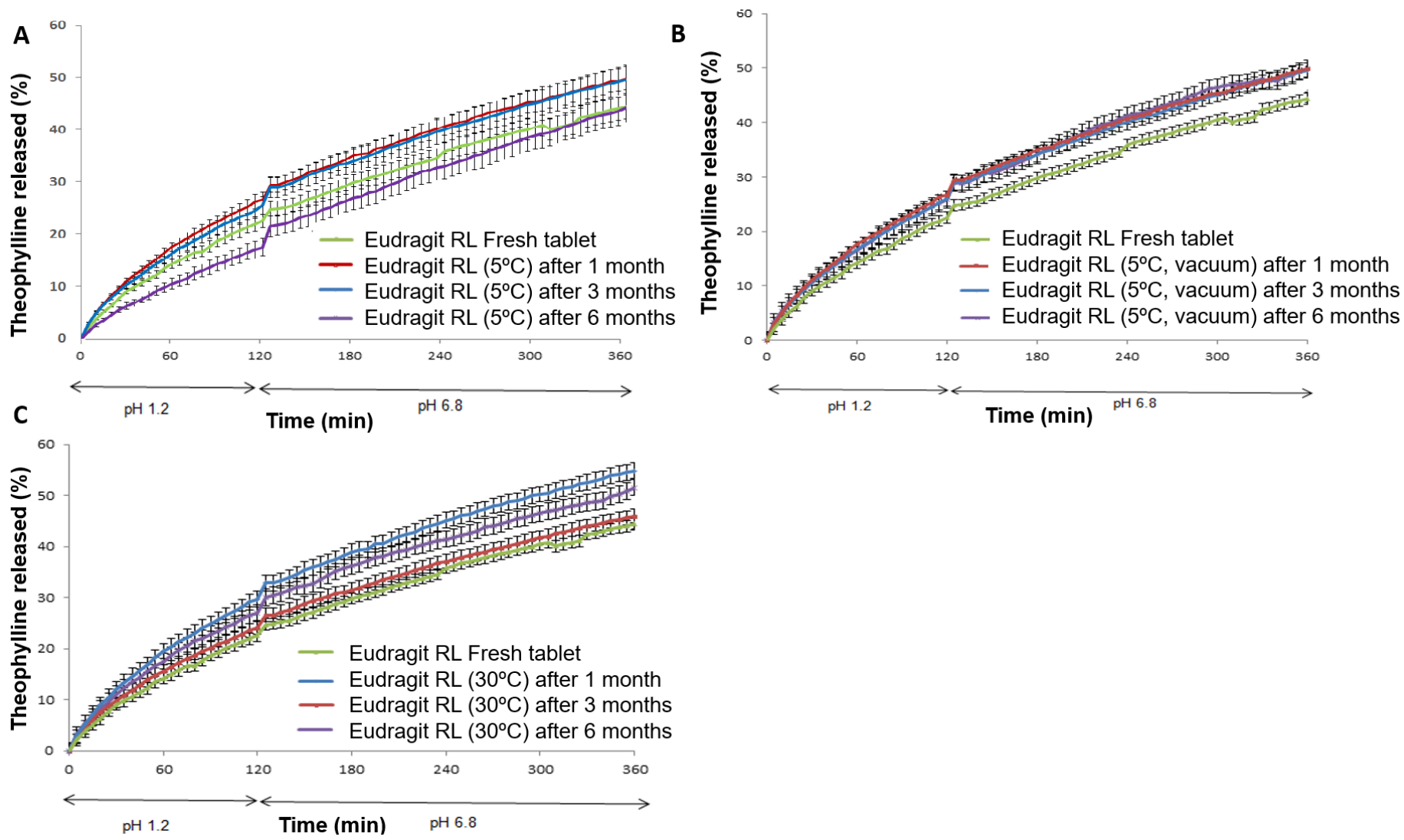


Fig. 10. The impact of the storage conditions on the *in-vitro* release profile of theophylline from the Eudragit RL-based 3D printed tablets.

printing temperatures).

Formulation/ Ratio (%)	HME Processing temp (°C)	HME Extrusion temp (°C)	Nozzle size (mm)	3D printing temp (°C)	Platform temp (°C)
PVP: TEC: Talc: Theo 50: 12.5: 27.5: 10	100	90	1.25	110	40
HPC.SSL: Triacetin: Theo 50: 5: 45	125	115	1.7	160	40
Eudragit L100-55: TEC: Talc 50: 16.67: 33.33	135	125	1	185	40
Eudragit S100: TEC: Talc 52.5: 22.5: 25	130	120	1.5	190	40
Eudragit RL: TEC: Theo 50: 5: 45	130	120	1.5	160	40
Eudragit EPO: TEC: Theo 50: 3.25: 46.75	100	90	1.25	135	45

Table 2. Impact of storage conditions on filament diameters, visual appearance and compatibility with printing process.

Filament	Filament/ Storage condition	Filament diameter (mm)		Compatibility with FDM 3D printing	Visual appearance after storage
		Before storage	After 6 months		
PVP-based	5 °C	1.50 ±0.04	1.53 ±0.03	✓ too flexible	No Change
	5 °C + Vac	1.50 ±0.01	1.48 ±0.02	✓ too flexible	No Change
	30 °C + 65% RH	1.37±0.09	N/A*	X Deformed	flattened
	30 °C + 65% RH + Vac	1.49±0.01	N/A*	X Deformed	flattened
HPC.SSL-based	5 °C	1.64 ± 0.04	1.63 ± 0.04	X too flexible	No Change
	5 °C + Vac	1.79 ± 0.01	1.69 ± 0.04	X too flexible	No Change
	30 °C/65% RH	1.58 ± 0.10	1.59 ± 0.13	X too flexible	No Change
	30 °C/65% RH + Vac	1.69 ± 0.05	N/A*	X Deformed	flattened
Eudragit L100-55-based	5 °C	1.67 ±0.03	1.67 ±0.04	✓	No Change
	5 °C + Vac	1.67 ±0.14	1.65 ±0.14	✓	No Change
	30 °C + 65% RH	1.61 ±0.05	1.77 ±0.06	✓	No Change
	30 °C + 65% RH + Vac	1.73 ±0.06	N/A*	X Deformed	flattened
Eudragit S100-based	5 °C	1.53 ±0.02	1.54 ±0.02	✓	No Change
	5 °C + Vac	1.61 ±0.08	1.62 ±0.05	✓	No Change

	30 °C + 65% RH	1.63 ±0.02	1.63 ±0.02	✓	No Change
	30 °C + 65% RH + Vac	1.62 ±0.03	1.62 ±0.03	✓	No Change
Eudragit RL-based	5 °C	1.59 ± 0.05	1.57 ± 0.03	✓	No Change
	5 °C + Vac	1.57 ± 0.01	1.59 ± 0.04	✓	No Change
	30 °C/65% RH	1.57 ± 0.01	1.55 ± 0.03	✓	No Change
	30 °C/65% RH + Vac	1.57 ± 0.04	N/A*	X Deformed	Flattened
Eudragit EPO-based	5 °C	1.59 ± 0.05	1.58 ± 0.03	✓	No Change
	5 °C + Vac	1.59 ± 0.01	1.61 ± 0.04	X Too flexible	No Change
	30 °C/65% RH	1.68 ± 0.04	1.66 ± 0.03	✓	No Change
	30 °C/65% RH + Vac	1.62 ± 0.04	N/A*	X Deformed	Flattened